Development of a robotic detection system for greenhouse pepper plant diseases

Noa Schor, Sigal Berman, Aviv Dombrovsky, Yigal Elad, Timea Ignat & Avital Bechar

Precision Agriculture
An International Journal on Advances in Precision Agriculture

ISSN 1385-2256
Volume 18
Number 3

Precision Agric (2017) 18:394-409
DOI 10.1007/s11119-017-9503-z

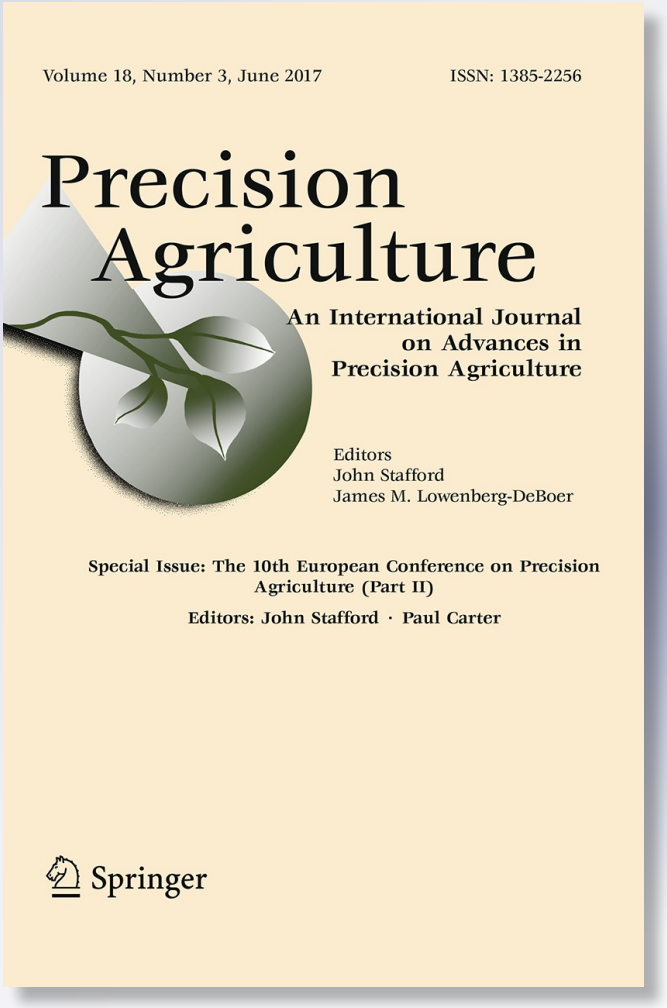

Springer

Precision Agric (2017) 18:394–409
DOI 10.1007/s11119-017-9503-z

Development of a robotic detection system for greenhouse pepper plant diseases

Noa Schor[1,2] · Sigal Berman[1] · Aviv Dombrovsky[3] · Yigal Elad[3] · Timea Ignat[2] · Avital Bechar[2]

Published online: 7 February 2017

Abstract Automation of disease detection and monitoring can facilitate targeted and timely disease control, which can lead to increased yield, improved crop quality and reduction in the quantity of applied pesticides. Further advantages are reduced production costs, reduced exposure to pesticides for farm workers and inspectors and increased sustainability. Symptoms are unique for each disease and crop, and each plant may suffer from multiple threats. Thus, a dedicated integrated disease-detection system and algorithms are required. The development of such a robotic detection system for two major threats of bell pepper plants: powdery mildew (PM) and *Tomato spotted wilt virus* (TSWV), is presented. Detection algorithms were developed based on principal component analysis using RGB and multispectral NIR-R-G sensors. High accuracy was obtained for pixel classification as diseased or healthy, for both diseases, using RGB imagery (PM: 95%, TSWV: 90%). NIR-R-G multispectral imagery yielded low classification accuracy (PM: 80%, TSWV: 61%). Accordingly, the final sensing apparatus was composed of a RGB sensor and a single-laser-beam distance sensor. A relatively fast cycle time (average 26.7 s per plant) operation cycle for detection of the two diseases was developed and tested. The cycle time was mainly influenced by sub-tasks requiring motion of the manipulator. Among these tasks, the most demanding were the determination of the required detection position and orientation. The time for task completion may be reduced by increasing the robotic work volume and by improving the algorithm for determining position and orientation.

✉ Avital Bechar
avital@volcani.agri.gov.il

[1] Department of Industrial Engineering and Management, Ben-Gurion University of the Negev, Beer-Sheva, Israel

[2] The Institute of Agricultural Engineering, Agricultural Research Organization, The Volcani Center, Beit Dagan, Israel

[3] The Institute of Plant Protection, Agricultural Research Organization, The Volcani Center, Beit Dagan, Israel

Keywords Disease detection · Multispectral imagery · RGB imagery · *Tomato spotted wilt virus* · Powdery mildew

Introduction

Markets for specialty crops are becoming increasingly challenging and demanding, threatening the long-term viability of crop growers (Lee et al. 2010). Greenhouses offer a controlled environment that can support optimal growth conditions and maximize yield. However, these conditions also favor the growth of many other organisms, such as weeds, insects, bacteria, fungi and viruses, which cause and transmit plant diseases. The impact of plant diseases on yield can be devastating and can lead to large potential annual losses for world food production (Oerke and Dehne 2004). To facilitate attaining production potential and to prevent significant yield losses, periodic and repetitive disease detection and monitoring during the plant's entire life cycle is essential (Pernezny et al. 2003; Elad et al. 2007). Disease containment along with a reduction in applied pesticides can only be achieved through early disease detection and identification of its foci. Improvements in both production quantity and quality, along with increased greenhouse productivity and sustainability, can be achieved through improvement of disease-detection procedures.

Today, in commercial greenhouses, disease detection is conducted manually by expert inspectors. As this relies on workforce availability and cost, the sampling resolution and rate are low, with about 20 arbitrary locations sampled per hectare (ha) in a fixed pattern where each plot is revisited every 7–10 days. The inspector walks about 20 km per day covering about 8 ha. Therefore, a designated inspector is required for every 70–80 ha of greenhouse. These limitations can lead to late detection and inability to contain a disease. As a precaution, even when symptoms are far below the thresholds that mandate pesticide application, repeated high doses of pesticide are often applied. Although disease distribution is typically centered in distinct locations, when a disease is identified pesticides are applied uniformly throughout the greenhouse. This leads to surplus use of pesticides, which not only increases costs but can also have a major environmental impact.

Automation of disease detection can alleviate these difficulties, leading to yield improvement along with a significant reduction in pesticide use (Franke and Menz 2007; Franke et al. 2009; Bock et al. 2010). In addition to reduced production costs, this will also lead to reduced exposure to pesticides for farm workers and inspectors, and increased sustainability (Hillnhuetter and Mahlein 2008). Plant diseases can affect various optical foliage characteristics and therefore, disease detection can be based on different spectral ranges (Lee et al. 2010). Disease detection based on image processing of foliage light reflection has been applied to many different diseases and cultivars (for reviews see Lee et al. 2010; Patil and Kumar 2011; Barbedo and Garcia 2013; Pujari et al. 2015). Methods based on fluorescence (Wetterich et al. 2016) or thermography (Oerke et al. 2011) can also be used for disease detection and have been extensively studied, but they are less relevant for a robotic detection system operating in the field due to cost, payload weight or required setup. Mobile robotic manipulators with various sensing capabilities offer an automation solution that is suitable for disease detection in greenhouses. However, comprehensive research on the development of such integrated robotic disease-detection systems for greenhouses is sparse, probably because the preliminary challenge of developing robust disease detection algorithms is still an open research question. Aerial platforms (West and

Kimber 2015) and ground mobile robotic platforms with fixed sensor configurations (Moshou et al. 2011; Pilli et al. 2014) have been tested for disease detection in open field crops. However, both solutions have inherent shortcomings in greenhouses. The maneuverability and flight duration of aerial systems within greenhouses is limited, and navigation and location cannot rely on GPS sensors since the construction can cause unpredictable errors, eliminating their main outdoor advantage. In greenhouses, position and orientation adaptation can significantly improve detection, especially early detection when symptoms are typically centered in distinct locations. However, for a fixed sensor configuration, position and orientation adaptation is not possible. Moreover, in fixed-configuration systems, a need for multiple disease detection can lead to a requirement for multiple detection positions and orientations, which tends to increase system complexity and cost, and hinder maneuverability. Therefore, a robotic disease-detection system for greenhouse pepper plants was developed based on the concept of a mobile robotic manipulator (Schor et al. 2015, 2016) which offers the required maneuverability and flexibility. To the best of the authors' knowledge, disease-detection systems based on a mobile robotic manipulator for specialty crops in greenhouses have not been previously developed.

Bell pepper (*Capsicum annuum*) is a high-value specialty crop grown mostly in greenhouses for fresh markets. It is cultivated worldwide and used as a food ingredient, spice and ingredient in medicine. The powdery mildew (PM) and the *Tomato spotted wilt* (TSWV) are two common threats of greenhouse-grown pepper plants (Pernezny et al. 2003; Kenyon et al. 2014). The PM fungi and the TSWV (a virus, causal organism) were selected due to their high disease severity in fruits and plants which significantly decreases fruit quality (Moury and Verdin 2012; Kenyon et al. 2014). As the characteristics of the diseases differ with respect to visible symptoms and outbreak regions, detection of these two threats during a single pass of a robotic system is challenging. The current research is the first to develop a robotic system for disease detection in greenhouse pepper plants (Schor et al. 2015). Monitoring of several diseases of pepper plants using a single monitoring system based on machine vision, and image-processing algorithms for TSWV and PM detection have not been previously reported.

TSWV is transmitted by at least eight species of thrips (Thysanoptera: Thripidae) (e.g., the western flower thrips *Frankliniella occidentalis*) (Pernezny et al. 2003) in a persistent and propagative manner (Fereres and Raccah 2015). Since 2004, TSWV isolates have overcome the resistance gene *Tsw* in pepper and the resistance gene *Sw-5* in tomato, making it difficult to manage (Margaria et al. 2004; Aramburu et al. 2010). In addition, TSWV infects a wide range of host plants from different botanical families and is therefore considered a major threat in many vegetable crops, e.g., tomato, tobacco, lettuce, pepper, papaya, eggplant, green beans, artichokes, broad beans and celery (Moury and Verdin 2012). Over 1 000 plant species experience severe losses due to the virus (Rosella et al. 1996). In pepper plants, TSWV causes a range of symptoms: sudden yellowing, mild mottling, mosaicking and browning of young leaves on the upper part of the plant, later become necrotic. Occasionally, ring-shaped spots appear on both leaves and fruit. TSWV causes heavy crop losses since fruit formed after infection display large necrotic streaks and spots, while younger fruit may develop necrotic symptoms (Avila et al. 2006). Early detection of TSWV in pepper plants is crucial, as it overcame plant resistance only recently (Crescenzi et al. 2013). Currently, there is no treatment for TSWV in pepper plants, and thus infected plants must be eradicated as soon as possible in order to prevent the secondary spread of the disease by the thrips vector. TSWV detection has used serology-based methods, e.g., enzyme-linked immunosorbent assay or by molecular based amplification

RT-PCR which is capable of providing an efficient diagnostic 14-21 days post-inoculation (Avila et al. 2006; Crescenzi et al. 2013). Such methods require leaves from the 'suspected plants' prior to the diagnostic assay. An additional disadvantage of these methods is that the selection of samples for testing has a critical influence on method reliability due to uneven distribution of TSWV in a greenhouse.

PM, caused by the fungus *Leveillula taurica*, is a serious threat to a very wide range of hosts, including tomato and pepper. The list of affected plants extends to more than 1 000 plant species (Zheng et al. 2013). Economic losses and specifically, yield losses of 2–4 kg m^{-2}, were reported for greenhouse pepper in British Columbia in 2002 due to heavy PM epidemics (Cerkauskas and Buonassisi 2003). Studies conducted in greenhouses and fields have shown that leaves infected with PM shed prematurely, resulting in reduced photosynthetic area, inhibition of fruit development, reduction in the number of flowers per plant and increased sunburn damage to exposed fruit (Elad et al. 2007). Pernezny et al. (2003) described the visible symptoms of PM in pepper plants as yellow–brown spots with whitish powdery mycelium, which typically appear first on the underside of older and lower leaves. Image-based detection algorithms have been developed for PM in wheat (Franke and Menz 2007), sugar beet (Rumpf et al. 2010; Mahlein et al. 2013) and grapevine (Bélanger et al. 2008; Oberti et al. 2014) using UV (Bélanger et al. 2008) and multispectral reflectance (Franke and Menz 2007; Oberti et al. 2014). Bélanger et al. (2008) measured UV-induced fluorescence to detect and quantify PM infection symptoms on grapevine leaves by investigating different emission/excitation wavelength combinations. They found that the ratios between blue and green fluorescence intensity in healthy and diseased areas of leaves are significantly different starting 3 days after infection. However, the developed UV-based detection method requires complex fluorescence excitation, complicating its implementation outside the laboratory. The potential of multispectral remote sensing for PM detection in wheat was presented by Franke and Menz (2007), who achieved a maximum classification accuracy of 88%. Oberti et al. (2014) investigated how the camera orientation can affect the sensitivity of PM detection in grapevine leaves using multispectral imaging. Overall results indicated that detection sensitivity generally increases with increasing angle of view, peaking for images acquired at 60°.

The robotic disease-detection system described herein was developed in a holistic manner, that is, system architecture, operation cycle and detection algorithms were developed in an integrated manner. It has been shown that early integration and testing of perception requirements can lead to improved system design and operation, in environments with taxing perception requirements (e.g., the agricultural environment) (Eizicovits et al. 2016). The current paper presents the development of the disease-detection apparatus and its integration into the robotic system's operation cycle.

Methodology

System design

The system includes three main components: a robotic manipulator, a custom-made end effector, and a sensory apparatus (Fig. 1). The sensory apparatus is comprised of a RGB camera (LifeCam NX-6000 WebCam, Microsoft, Redmond, WA, USA) with a resolution of 1600 × 1200 pixels, a NIR-R-G multispectral camera (ADC Lite, 520–920 nm,

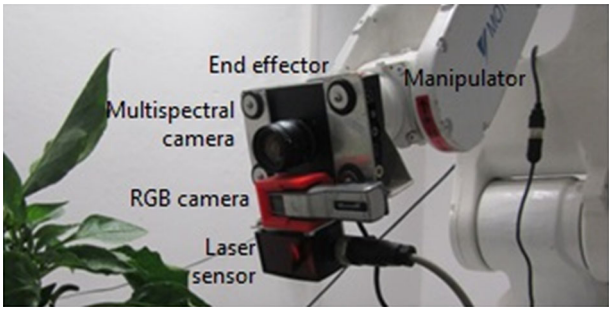

Fig. 1 The robotic detection system

equivalent to TM2, TM3 and TM4, Tetracam, Chatsworth, CA, USA) with a resolution of 2048 × 1536 pixels, and a single-laser-beam distance sensor (DT35, SICK, Waldkirch, Germany). The sensor devices are mounted on the end effector, which is attached to a six degrees-of-freedom manipulator (MH5L, Motoman, Yaskawa, Eschborn, Germany). Parts of the end effector were fabricated using a 3D printing system (Trio, CubeX, Rock Hill, SC, USA). These parts were designed to align the sensor devices in parallel, making them coaxial with the manipulator's tool center point (TCP). To simplify the initial development stages and as there are platforms capable of autonomously driving through greenhouse isles (e.g., Van Henten et al. 2002), the robotic arm was placed near a conveyor belt carrying pots with plants simulating the movement of the system in a greenhouse plot. The manipulator will be mounted on a mobile platform at a later stage during field-testing.

Sensory apparatus

Both RGB and multispectral NIR-R-G sensors are readily available (such as Canon, Microsoft WebCam, Tetracam, which are considered low-cost off-the-shelf products) and can be integrated with a robotic manipulator; RGB sensors are typically less expensive. Multispectral NIR-R-G sensors are commonly applied to disease detection as many diseases are characterized by changes in reflectance properties in this range of bandwidths. To determine the required sensory apparatus, the ability of each sensor to correctly classify pixels as diseased or healthy, for PM and for TSWV was tested. Two cameras were compared: an RGB camera (PowerShot SX210 IS, Canon, Melville, NY, USA) with a resolution of 4320 × 3240 pixels, and a NIR-R-G multispectral camera (ADC Lite, similar to the one included in robotic sensory apparatus).

PM-detection algorithm

A preliminary analysis of raw pixel values (either R, G, and B or the multispectral NIR, R, and G channels) did not yield clear separation between healthy and diseased pixels. Therefore, principal component analysis (PCA) was conducted on the raw pixel values. A binary classification (healthy or diseased) was determined for each pixel, based on the two main principal components. Classification thresholds were determined a priori using linear discriminant analysis (LDA) and quadratic discriminant analysis (QDA). Since prior work on PM detection identified specific NIR-R-G multispectral indices for grapevine PM (Oberti et al. 2014), these indices were also computed.

TSWV-detection algorithm

A preliminary analysis of both raw pixel values and PCA of these values did not yield good separation for either sensor. Visual examination indicated that for TSWV, the differences between symptom color and leaf color are small, and leaf veins and disease symptoms have similar color levels. Therefore, a leaf vein extraction algorithm was implemented. The algorithm was based on the Savitzky–Golay smoothing and differentiation algorithm (Savitzky and Golay 1964) followed by application of multilevel image thresholds using Otsu's (1979) method and morphological filters (e.g., area open and dilate). Preliminary analysis confirmed that this stage is required for TSWV and that for PM, it is not. PCA was conducted after leaf vein removal and a binary classification (healthy or diseased) was determined for each pixel, based on the two main principal components. Classification thresholds were determined a priori using LDA and QDA.

System operation cycle

To attain high sampling resolution and large area coverage, detection cycle time should be minimized. To shorten the cycle time, disease detection is performed during a single pass of the robot manipulator around the plant. To further shorten operation cycle time, TSWV detection is done first because currently, there is no cure for TSWV and if detected, the plant is immediately marked for eradication; detection of PM on that plant is therefore not required. Each cycle (Fig. 2) starts with a TSWV detection task which, in the case of a negative result, is followed by a PM detection task. To avoid collision with the plant when moving from one task to another and when the manipulator moves from the TSWV detection position and orientation to the PM detection position and orientation, and from this position and orientation to the next plant, the manipulator moves through an

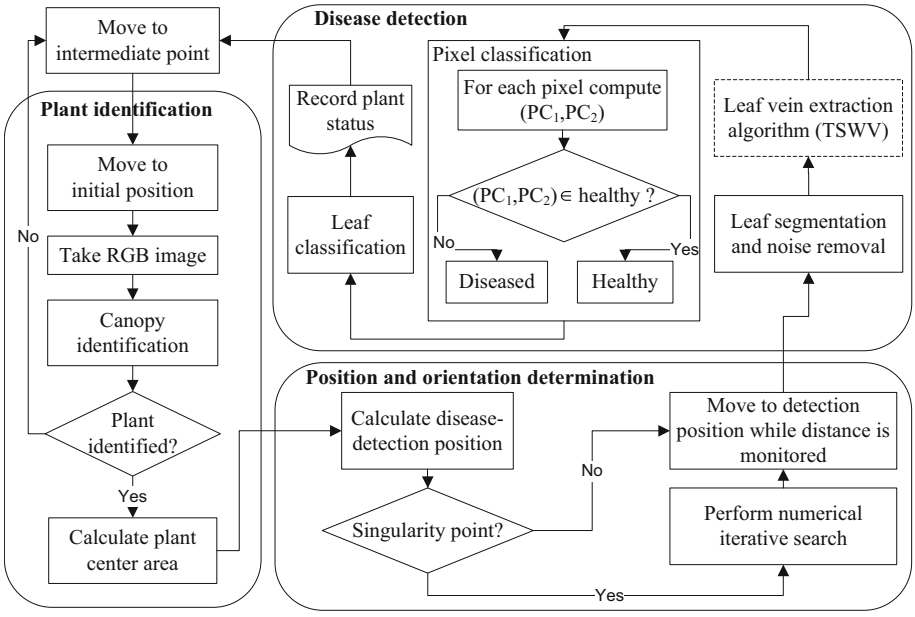

Fig. 2 Operation cycle

intermediate point ensuring motion outside the plant foliage. The motion planner calculates a straight path to and from the intermediate point using the manipulator's kinematic model. Each detection task includes three subtasks: plant identification, position and orientation determination and disease detection.

Plant identification

For plant identification, the end effector moves to an initial position and orientation determined a priori. For TSWV detection, the initial position and orientation is above the plant (sensor apparatus facing down), whereas for PM detection, it is alongside the plant (sensor apparatus facing sideways toward the plant). A RGB image is acquired from the initial position and orientation and the plant canopy is detected using blob analysis and morphological filters. The center of the plant, i.e., the center of the green blob, is calculated (Fig. 3). The central area of the plant is defined as a 16 × 16 pixel, bounding square around the center of the plant.

Position and orientation determination

The position and orientation for disease detection is calculated based on the central area and the kinematic model of the robot. Since the required TSWV detection position and orientation may be close to the manipulator singularity point, in which the shoulder and elbow links of the manipulator are fully aligned and the inverse kinematic equations cannot be solved analytically in this region, a numerical iterative search is implemented. The objective of the iterative search is to position the TCP within the central area (Fig. 3a) and it is executed by fixed roll-and-pitch movements. The direction of the joint movements (left or right and up or down) is determined according to the concurrent TCP position with respect to the plant center area. For PM detection, the detection position and orientation can be computed analytically. The manipulator moves toward the determined detection position and orientation while using the laser sensor to continuously monitor the distance to the plant canopy and ensure that a distance of 210–270 mm from the plant foliage is reached to obtain the required leaf resolution. The distance-control algorithm was developed under the hypothesis that the closest object to the end effector is the plant, and

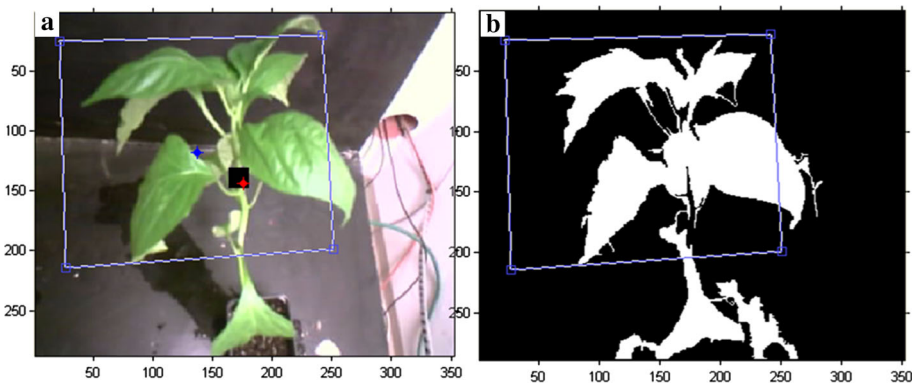

Fig. 3 Initial position and orientation as seen from the RGB camera mounted on the robotic arm. **a** RGB image with plant center area (*black box*) and TCP (*red dot*). **b** Binary image (Color figure online)

therefore the laser sensor indeed measures the distance to the plant foliage (either top or side). Multiple distance measurements are executed since a single measurement may miss the plant. Once a plant is identified and the camera position and orientation are established, the disease-detection procedure is initiated.

Disease detection

Detection is performed at leaf level, and therefore before the detection algorithms start, the leaf is segmented and background noise is removed based on blob analysis and morphological filters. Several two-stage disease-detection algorithms were implemented using the two spectral ranges: RGB and multispectral NIR-R-G. In the first stage, each pixel is classified using PCA as either diseased or healthy (Schor et al. 2015, 2016). In the second stage, leaf condition is determined based on the ratio of diseased pixels. For TSWV detection, leaf condition is determined as either healthy or diseased since, even at an early stage of the disease, the plant is marked for eradication. For PM detection, the leaf is marked as healthy or with low or medium disease severity to direct the treatment (Schor et al. 2016).

Experiments

Disease detection experiments

The analysis was conducted using a computer equipped with an Intel Core i7-3632QM 2.2 GHz processor with turbo boost up to 3.2 GHz (CPU) and 8 GB RAM with Windows 8 (64-bit) operating system. The detection algorithms were implemented using Matlab R2013b (Mathworks, Natick, MA, USA) and statistical analysis was conducted using IBM SPSS statistics 19 (IBM, Armonk, NY, USA). Pixel classification quality was determined based on 10×2 cross-validation. Results are presented using overall accuracy, which reflects the ratio of correct classifications (both healthy and diseased):

$$accuracy = \frac{TP + TN}{TP + FP + FN + FN} \quad (1)$$

where healthy is regarded as positive and diseased is regarded as negative. *TP* is true positive and *FN* is false negative.

Sweet bell pepper plants (Hazera Genetics) were obtained from a commercial nursery (Hishtil, Ashkelon, Israel) 40–50 days after seeding. The plants were transplanted into 36 pots containing soil and potting medium and were fertigated proportionally with drippers 2–3 times per day with 5:3:8 NPK fertilizer (nitrogen (N), phosphorus (P) and potassium (K)), allowing for 25–50% drainage. Irrigation water was planned for total N, P and K concentrations of 120, 30, and 150 mg l^{-1}, respectively; electrical conductivity of water (EC) was 2.2 dS m^{-1}. Plants were maintained at 20–30 °C in a pest- and disease-free greenhouse where their healthy status was ascertained visually by plant pathologists (Schor et al. 2015).

The 36 plants were divided into two subsets positioned in two different greenhouses: 24 plants for PM detection and 12 for TSWV detection. Images of the plants were acquired in the greenhouses at noon time with the RGB and the NIR-R-G cameras (Fig. 4). Of the 24 plants from the PM subset, 12 were infected with PM 4 months after transplanting. Starting with the occurrence of the first symptom reported by the plant pathologists (2 days after

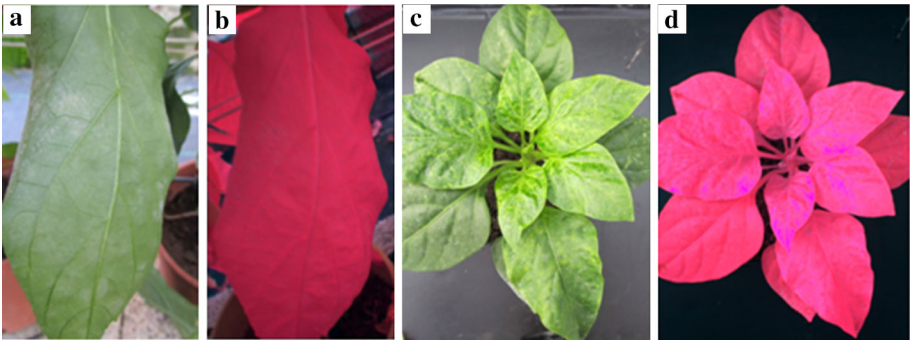

Fig. 4 Leaves with disease symptoms. PM forms on the underside of leaves: **a** RGB image and **b** NIR-R-G image. TSWV-infected pepper plants: **c** RGB image and **d** NIR-R-G image (Schor et al. 2015)

inoculation), images of both sides of 24 selected leaves (12 healthy and 12 diseased), each from a different plant, were acquired every 3 days over a 17-day period. Three leaves (two healthy and one diseased) were torn unintentionally during data collection and their images were discarded. Of the 12 plants from the TSWV subset, six were infected with TSWV 2 weeks after transplanting. Images of the top and sides of the plants were taken daily in the greenhouse for 15 consecutive days (days 3–17 after inoculation). As the plants were small during the data-collection period, images of plants rather than leaves were taken. For both diseases, in addition to disease intensity, the images show pigmentation due to possible interfering nutritional or physiological disorders.

TSWV and PM symptoms in all images were manually marked by plant pathologists and each pixel was classified as healthy or diseased by marking polygons of diseased areas in the images. Leaves were classified as either healthy or diseased and disease severity was additionally graded as low, medium or high. The pathologists also classified the condition of each leaf on every recorded day. For PM leaf classification, the pathologists used the images of both sides of the leaf. TSWV symptoms typically appear at the top of the plant. Visual inspection by the plant pathologists verified that TSWV symptoms were indeed undetectable from the side-view images. Therefore, only the images of the top of the plant were used. Within the calibration images, subset areas were extracted from infected areas identified by the plant pathologists. Sub-set areas were also extracted from healthy plants. The number of regions of interest (ROIs) for each class was chosen to obtain a balanced distribution between healthy and diseased tissue at different stages of disease progression (Schor et al. 2015). The selected ROIs from the calibration set were used to tune the disease-detection model and to train the classification parameters.

Operation cycle experiment

System operation cycle time is a critical feature in facilitating system acceptance and its economic justification. Setting the capacity of a human inspector as the minimal baseline capacity for the robotic system, a minimum baseline for the required cycle time can be computed. Indeed, this baseline does not ensure that the system will be economically feasible or acceptable to the farmers, but it can give a general appreciation of the attained results. During an 8 h work shift, an expert inspector examines about 160 plants (20 plants ha^{-1}, 8 ha per day) and walks about 20 km. Mobile robots have been tested navigating in a greenhouse at speeds of 1.2 m s^{-1} (González et al. 2009). Taking a conservative average

speed of 1 m s^{-1}, the robot would require 5.56 h to travel a distance of 20 km. This would leave 2.44 h for examination of 160 plants, which means 55 s per plant.

The system operation cycle time was tested in an indoor laboratory environment. The plants were positioned on a conveyor belt with black background to simplify plant-identification and background-removal procedures. In these tests, the plants were stationary during the detection process. The detection system was controlled by a computer equipped with an Intel Pentium Dual E2180 2 GHz processor (CPU) and 2 GB RAM with Windows XP (32-bit) operating system. The algorithms were implemented using Matlab R2009b (Mathworks). Three plant locations (770, 900 and 1050 mm away from the robotic system base in the workspace co-ordinates), and three end-effector velocities (5, 15 and 25% of maximum speed) were tested. Each condition was executed for 10 healthy plants. Overall, there were 90 runs of the system. Execution time was computed for each sub-task to determine the most time-consuming sub-task. Cycle time was defined as the sum of all sub-task times.

Results

TSWV detection

A total of 72 RGB images and 72 leaf-matched NIR-R-G multispectral images were analyzed (36 healthy and 36 infected leaves). Images of infected leaves were taken from plants with leaves marked as having low and medium severity of TSWV (18 low and 12 medium), 12–17 days after inoculation. Images of healthy leaves were taken from day-matched leaves. Six images were excluded from each sensor set: three of infected plants taken 12 days after inoculation where visible symptoms had not yet appeared, and three taken 14, 15 or 16 days after inoculation which the plant pathologist misdiagnosed.

PCA-based pixel classification of RGB images achieved accuracies of 85.6 and 83.5% using QDA and LDA, respectively (Fig. 5a). PCA-based pixel classification of NIR-R-G images achieved accuracies of 60.0 and 61.1% using QDA and LDA, respectively (Fig. 5b).

PM detection

A total of 45 RGB images and 45 leaf-matched NIR-R-G multispectral images were analyzed from the PM database (15 healthy leaves and 30 infected leaves each for RGB and multispectral NIR-R-G). Images of the upper side, which is more visible, of infected leaves marked as having low or medium severity of PM (11 low and 19 medium) were analyzed. Images of the underside of leaves were not analyzed since they are not visible to the robotic disease detection system.

PCA-based pixel classification of RGB images achieved accuracies of 95.2 and 94.8% using QDA and LDA, respectively (Fig. 6a). PCA-based pixel classification of NIR-R-G images achieved accuracies of 71.6 and 79.9% using QDA and LDA, respectively (Fig. 6b).

The spectral indices for the multispectral NIR-R-G sensor suggested by Oberti et al. (2014) for PM detection in grapevine were examined for a sample of healthy and infected pixels in pepper plants (Fig. 7). Separation accuracies of 59.0 and 66.3% using QDA and LDA, respectively, were attained.

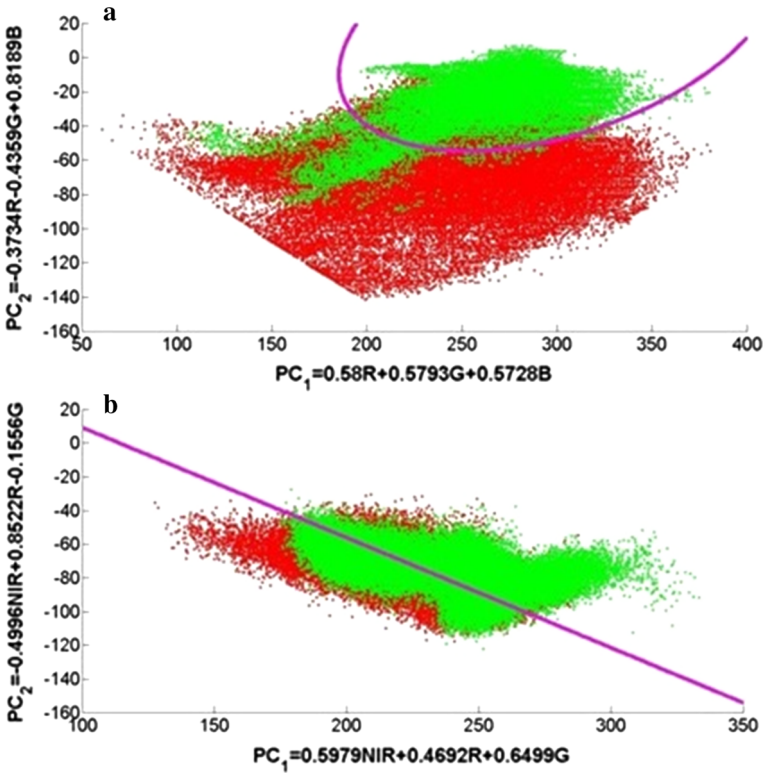

Fig. 5 First (PC1) versus second (PC2) principal components of R, G and B variables (**a**) and NIR, R and G variables (**b**) for TSWV-infected and healthy pepper plants. Altogether, 60 000 healthy (*green*) and 60 000 diseased (*red*) pixels are displayed. The *pink solid lines* represent the functions separating the decision regions (Color figure online)

Operation cycle

The system operated continuously throughout the trials. Average cycle time (sub-tasks detailed in Fig. 8) were 42.9, 26.7 and 24.3 s for end-effector velocities of 5, 15 and 25%, respectively.

Execution time of all tasks, including manipulator motion, except position and orientation determination for TSWV, decreased considerably when the manipulator speed was increased from 5 to 15%. The execution time continued to decrease but at a much lower rate when the manipulator speed was further increased from 15 to 25%. For TSWV position and orientation determination, execution times were similar at all velocities. Execution times of the disease detection tasks (which did not include manipulator motion) were negligible with respect to the execution time of the tasks that included manipulator motion (TSWV detection: 0.06 s and PM detection: 0.06 s).

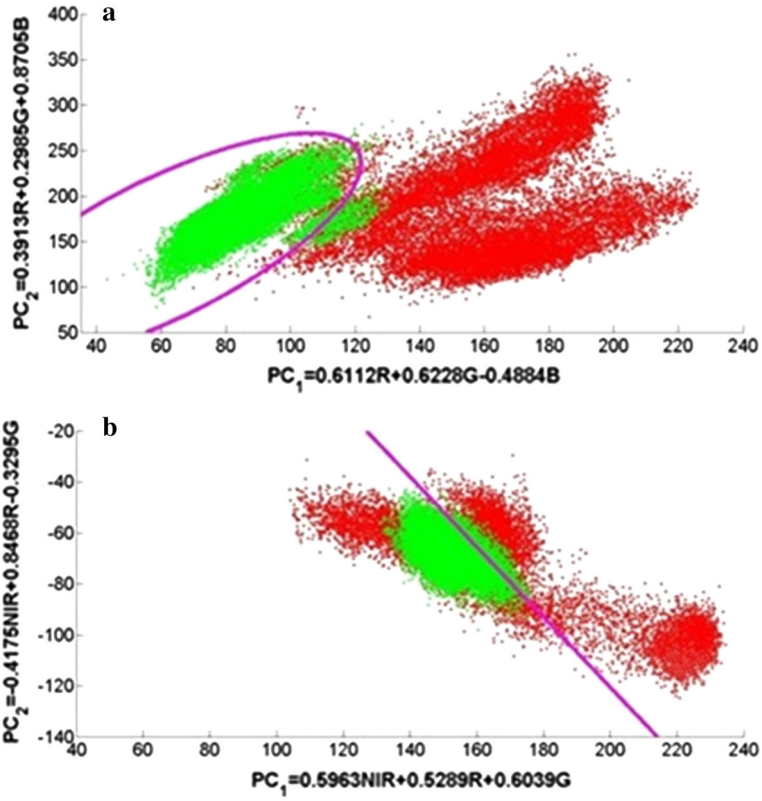

Fig. 6 First (PC1) versus second (PC2) principal components of R, G and B variables (**a**) and NIR, R and G variables (**b**) for PM-infected and healthy pepper plants. Altogether, 20 000 healthy (*green*) and 20 000 diseased (*red*) pixels are displayed. The *pink solid lines* represent the functions separating the decision regions (Color figure online)

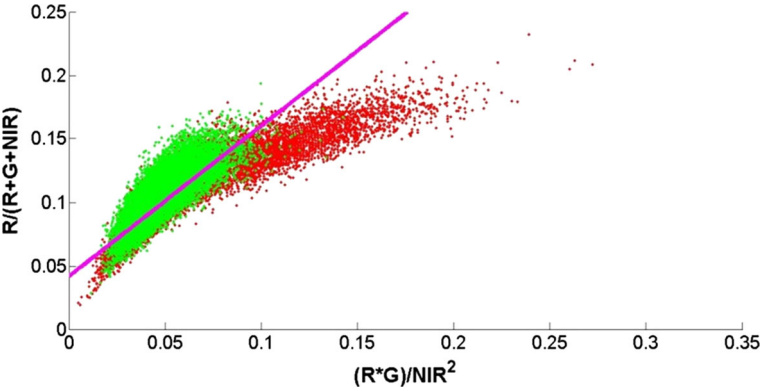

Fig. 7 First index ($R*G/NIR^2$) versus second index ($R/(R + G + NIR)$) of NIR, R and G variables for PM-infected and healthy pepper plants. Altogether, 20 000 healthy (*green*) and 20 000 diseased (*red*) pixels are displayed. The *pink solid lines* represent the functions separating the decision regions (Color figure online)

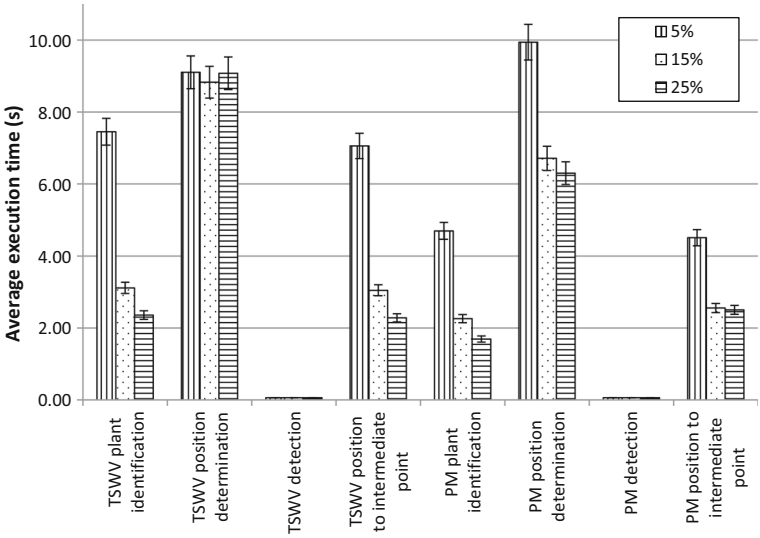

Fig. 8 Average execution time per subtask at end-effector velocities of 5, 10 and 15%. *Error bars* represent standard deviations

Discussion

For PM, results show that the spectral indices developed for grapevine (Oberti et al. 2014) are not applicable to bell pepper plants. PM has different symptoms and different progression characteristics (color, pattern, growth region, etc.) in different species, e.g., grapevine and bell pepper plants. This is in line with the need to develop more integrated crop- and pest-management strategies, as argued by Kenyon et al. (2014).

A high accuracy of pixel classification was obtained for both diseases using RGB imagery (PM: 95%, TSWV: 86%). In contrast, using NIR-R-G multispectral imagery resulted in low classification accuracy for both diseases (PM: 80%, TSWV: 61%). Thus, RGB imagery is clearly superior to NIR-R-G multispectral imagery for the current application. The results imply that some of the information regarding the diseases is contained in the blue channel, which does not exist in the multispectral camera. It has been shown for several diseases of sugar beet leaves that a combination of data from multispectral and RGB sensors can lead to highly accurate classification results (Bauer et al. 2011). However, it is not clear whether this is also the case for pepper plants. According to the results, a high-resolution RGB camera (e.g. the camera used for constructing the database) should be integrated into the sensing apparatus. Further tests will determine whether this camera can be used alone or installed alongside the multispectral camera.

The high pixel classification success using the RGB input indicates that this input can be used to determine leaf condition with a two-stage classification algorithm. In the first stage, pixel state is determined as healthy or diseased as described above and, in the second stage, leaf condition is determined based on the rate of diseased pixels in the leaf (Schor et al. 2016). For TSWV detection, the affected (top) side of the leaf is directly visible to the camera. Accordingly, for TSWV, PCA-based leaf-condition classification achieved high accuracy (90%). For PM detection, disease development starts on the underside of the leaf. Therefore, while detection is indeed possible using the top side of the leaf, for early

detection, the underside should be exposed. Consequently in the experiment, when only the upper side of the leaf was used, PM detection accuracy was low (64.3%) (Schor et al. 2016).

Results are very encouraging as the attained cycle time was lower than the calculated required baseline. However, the experiment was conducted in a simplified laboratory environment, e.g., the use of a conveyer belt rather than mounting the manipulator on a mobile platform or the black background used to simplify plant-identification and background-removal procedures. These made the disease detection task easier, and reduced cycle time. The greenhouse environment is unstructured and complex, as it includes obstacles, background noise and varying illumination. Conducting disease detection in such an environment will require sophisticated algorithms for motion control, path planning and additional image processing. This, in turn might extend cycle time. However, results also showed that cycle time can be further reduced in a straightforward manner. For TSWV detection, execution time does not change with manipulator speed. This indicates that the execution time is mainly influenced by the iterative numerical search for the inverse kinematic solution. Using a manipulator with a different work volume, for which an analytical solution exists for the inverse kinematic equations, could considerably shorten execution time. Although for PM, the execution time of the position and orientation detection task was shorter than for TSWV, this was the longest sub-task for both diseases. During position and orientation detection, the robot moves while operating the laser sensor to determine the distance from the plant. Improving the initial position and orientation estimation, along with improvements to the control cycle are expected to reduce the execution time of these tasks. Execution time of tasks that include motion is reduced when manipulator speed is increased, but this reduction is smaller as speed becomes higher, due to the manipulator acceleration and motion profile. According to the results, there is little to be gained by increasing manipulator speed beyond the tested speed of 25%. Similarly, results show that improving the efficiency of the disease detection algorithms will not significantly affect the overall execution time.

Conclusions

The current research targeted the development of a robotic disease detection system for two diseases of greenhouse pepper plants. Results of examining RGB and multispectral sensors for detection showed that it is important to include an RGB sensor as part of the disease detection sensor suite. Such a sensor should be added to the sensor apparatus either instead of, or alongside the multispectral sensor. Inclusion of both sensors should be carefully scrutinized, as it will increase system cost and will increase end-effector size, which may mandate a change in path to avoid collisions with the plants.

Investigation of the operation cycle indicated that the cycle time required for economic justification may be attainable. Results indicated that the structure and size of the manipulator should be re-examined in view of the position and orientation required for TSWV detection. Results also indicated that, for the examined system, the main reduction in cycle time can be expected from improvement of the position and orientation determination sub-task for both TSWV and PM.

Acknowledgements This research was supported by the Helmsley Charitable Trust through the Agricultural, Biological and Cognitive Robotics Initiative of Ben-Gurion University of the Negev and the Chief

Scientist Fund of the Ministry of Agriculture. The authors would like to thank Prof. Dan G. Blumberg for use of the multispectral camera.

References

Aramburu, J., Galipienso, L., Soler, S., & López, C. (2010). Characterization of Tomato spotted wilt virus isolates that overcome the Sw-5 resistance gene in tomato and fitness assays. *Phytopathologia Mediterranea, 49,* 342–351.

Avila, Y., Stavisky, J., Hague, S., Funderburk, J., Reitz, S., & Momol, T. (2006). Evaluation of *Frankliniella bispinosa* (Thysanoptera: Thripidae) as a vector of the Tomato spotted wilt virus in pepper. *Florida Entomologist, 89*(2), 204–207.

Barbedo, A., & Garcia, J. (2013). Digital image processing techniques for detecting, quantifying and classifying plant diseases. *SpringerPlus, 2,* 660. doi:10.1186/2193-1801-2-660.

Bauer, S. D., Kore, F., & Forstner, W. (2011). The potential of automatic methods of classification to identify leaf diseases from multispectral images. *Precision Agriculture, 12,* 361–377.

Bélanger, M. C., Roger, J. M., Cartolaro, P., Viau, A. A., & Bellon-Maurel, V. (2008). Detection of Powdery mildew in grapevine using remotely sensed UV-induced fluorescence. *International Journal of Remote Sensing, 29*(6), 1707–1724.

Bock, C. H., Poole, G. H., Parker, P. E., & Gottwald, T. R. (2010). Plant disease severity estimated visually, by digital photography and image analysis, and by hyperspectral imaging. *Critical Reviews in Plant Science, 29,* 59–107.

Cerkauskas, R. F., & Buonassisi, A. (2003). First report of Powdery mildew of greenhouse pepper caused by *Leveillula taurica* in British Columbia, Canada. *Plant Disease, 87*(9), 1151.

Crescenzi, A., Viggiano, A., & Fanigliulo, A. (2013). Resistance breaking tomato spotted wilt virus isolates on resistant pepper varieties in Italy. *Communications in Agricultural and Applied Biological Sciences, 78*(3), 609–612.

Eizicovits, D., Van Tuijl, B., Berman, S., & Edan, Y. (2016). Integration of perception capabilities in gripper design using graspability maps. *Biosystems Engineering, 146,* 98–113.

Elad, Y., Messika, Y., Brand, M., Rav David, D., & Sztejnberg, A. (2007). Effect of microclimate on *Leveillula taurica* powdery mildew of sweet pepper. *Phytopathology, 97*(7), 813–824.

Fereres, A., & Raccah, B. (2015). Plant virus transmission by insects. *Encyclopedia of Life Sciences*. doi: 10.1002/9780470015902.a0000760.pub3

Franke, J., Gebhardt, S., Menz, G., & Helfrich, H. P. (2009). Geostatistical analysis of the spatiotemporal dynamics of powdery mildew and leaf rust in wheat. *Phytopathology, 99,* 974–984.

Franke, J., & Menz, G. (2007). Multi-temporal wheat disease detection by multi-spectral remote sensing. *Precision Agriculture, 8*(3), 161–172.

González, R., Rodríguez, F., Sánchez-Hermosilla, J., & Donaire, J. G. (2009). Navigation techniques for mobile robots in greenhouses. *Applied Engineering in Agriculture, 25*(2), 153–165.

Hillnhuetter, C., & Mahlein, A. K. (2008). Early detection and localisation of sugar beet diseases: new approaches. *Gesunde Pflanzen, 60,* 143–149.

Kenyon, L., Kumar, S., Tsai, W. S., & Hughes, J. A. (2014). Virus diseases of peppers (*Capsicum* spp.) and their control. *Advances in Virus Research, 90,* 297–354.

Lee, W. S., Alchanatis, V., Yang, C., Hirafuji, M., Moshou, D., & Li, C. (2010). Sensing technologies for precision specialty crop production. *Computers and Electronics in Agriculture, 74,* 2–33.

Mahlein, A. K., Rumpf, T., Welke, P., Dehne, H. W., Plumer, L., Steiner, U., et al. (2013). Development of spectral indices for detecting and identifying plant diseases. *Remote Sensing of Environment, 128,* 21–30.

Margaria, P., Ciuffo, M., & Turina, M. (2004). Resistance breaking strain of Tomato spotted wilt virus (Tospovirus; Bunyaviridae) on resistant pepper cultivars in Almería, Spain. *Plant Pathology, 53,* 795.

Moshou, D., Bravo, C., Oberti, R., West, J. S., Ramon, H., Vougioukas, S., et al. (2011). Intelligent multi-sensor system for the detection and treatment of fungal diseases in arable crops. *Biosystems Engineering, 108*(4), 311–321.

Moury, B., & Verdin, E. (2012). Viruses of pepper crops in the Mediterranean basin: a remarkable stasis. *Advances in Virus Research, 84,* 127–162.

Oberti, R., Marchi, M., Tirelli, P., Calcante, A., Iriti, M., & Borghese, A. N. (2014). Automatic detection of Powdery mildew on grapevine leaves by image analysis: Optimal view-angle range to increase the sensitivity. *Computers and Electronics in Agriculture, 104,* 1–8.

Oerke, E. C., & Dehne, H. W. (2004). Safeguarding production losses in major crops and the role of crop protection. *Crop Protection, 23,* 275–285.

Oerke, E. C., Froehling, P., & Steiner, U. (2011). Thermographic assessment of scab disease on apple leaves. *Precision Agriculture, 12*(5), 699–715.

Otsu, N. (1979). A threshold selection method from gray-level histograms. *IEEE Transactions on Systems, Man, and Cybernetics, 9*(1), 62–66.

Patil, J. K., & Kumar, R. (2011). Advances in image processing for detection of plant diseases. *Journal of Advanced Bioinformatics Applications and Research, 2*(2), 135–141.

Pernezny, K. L., Roberts, P. D., Murphy, J. F., & Goldberg, N. P. (2003). *Compendium of pepper diseases*. Wisconsin: American Phytopathological Society.

Pilli, S. K., Nallathambi, B., George, S. J., & Diwanji, V. (2014). eAGROBOT—A robot for early crop disease detection using image processing. In *Proceedings of the IEEE International Conference on Electronics and Communication Systems* (pp. 1–6). New York: IEEE.

Pujari, J. D., Yakkundimath, R., & Byadgi, A. S. (2015). Image processing based detection of fungal diseases in plants. In *Proceedings of the International Conference on Information and Communication Technologies* (pp. 1802–1808). Amsterdam, The Netherlands: Elsevier Science.

Rosella, S., Jose Diez, M., & Nuez, F. (1996). Viral diseases causing the greatest economic losses to the tomato crop. I. The Tomato spotted wilt virus—a review. *Scientia Horticulturae, 67*(3–4), 117–150.

Rumpf, T., Mahlein, A. K., Steiner, U., Oerke, E. C., Dehne, H. W., & Plumer, L. (2010). Early detection and classification of plant diseases with Support Vector Machines based on hyperspectral reflectance. *Computers and Electronics in Agriculture, 74*(1), 91–99.

Savitzky, A., & Golay, M. J. E. (1964). Smoothing and differentiation of data by simplified least squares procedures. *Analytical Chemistry, 36*(8), 1627–1639.

Schor, N., Bechar, A., Ignat, T., Dombrovsky, A., Elad, Y., & Berman, S. (2016). Robotic disease detection in greenhouses: Combined detection of Powdery mildew and Tomato spotted wilt virus. *IEEE Robotics and Automation Letters, 1*(1), 354–360.

Schor, N., Berman, S., Dombrovsky, A., Elad, Y., Ignat, T., & Bechar, A. (2015). A robotic monitoring system for diseases of pepper in greenhouse. In Stafford, J. V. (Ed.) *Proceedings of the 10th European Conference on Precision Agriculture* (pp. 627–634). Wageningen, The Netherlands: Wageningen Academic Publishers.

Van Henten, E. J., Hemming, J., Van Tuijl, B. A. J., Kornet, J. G., Meuleman, J., Bontsema, J., et al. (2002). An autonomous robot for harvesting cucumbers in greenhouses. *Autonomous Robots, 13*(3), 241–258.

West, J. S., & Kimber, R. B. E. (2015). Innovations in air sampling to detect plant pathogens. *Annals of Applied Biology, 166*(1), 4–17.

Wetterich, C. B., Neves, R. F. O., Belasque, J., & Marcassa, L. G. (2016). Detection of citrus canker and Huanglongbing using fluorescence imaging spectroscopy and support vector machine technique. *Applied Optics, 55*(2), 400–407.

Zheng, Z., Nonomura, T., Appiano, M., Pavan, S., Matsuda, Y., Toyoda, H., et al. (2013). Loss of function in Mlo orthologues reduces susceptibility of pepper and tomato to powdery mildew disease caused by *Leveillula taurica*. *PLoS One*. doi:10.1371/journal.pone.0070723.